

## Kinetics of phase separation in polymer-solvent mixtures

Jitendra Sharma and Sanjay Puri

*School of Physical Sciences, Jawaharlal Nehru University, New Delhi, 110067, India*

(Received 19 December 2000; published 26 July 2001)

We investigate the kinetics of phase separation in systems with a strong asymmetry in the mobility. This simple model system mimics the segregation kinetics of polymer-solvent mixtures, where the polymer-rich phase forms a low-mobility gel. We obtain detailed numerical results for this model, both without and with thermal noise. In the absence of thermal noise, we find that domain growth is slowed down drastically when the low-mobility phase percolates the system. However, thermal noise restores rapid domain growth through a Brownian coalescence mechanism.

DOI: 10.1103/PhysRevE.64.021513

PACS number(s): 64.70.Dv, 64.60.-i

### I. INTRODUCTION

Consider a binary mixture (AB), which is in a homogeneous state at a high temperature. If this system is rapidly quenched below the coexistence curve, the preferred equilibrium state is one where the components are segregated. The temporal evolution of the unstable homogeneous mixture to a phase-separated state has received much attention in the literature [1]. Typically, the mixture segregates into domains which are enriched in either component. These domains coarsen with time and are usually characterized by a growing time-dependent length scale  $L(t)$ , where  $t$  is the time after the quench. A direct consequence of the existence of a unique length scale is the dynamical scaling of the correlation function [2], i.e.,

$$C(\vec{r}, t) \equiv \langle \psi(\vec{R}, t) \psi(\vec{R} + \vec{r}, t) \rangle - \langle \psi(\vec{R}, t) \rangle \langle \psi(\vec{R} + \vec{r}, t) \rangle \\ = g\left(\frac{r}{L(t)}\right), \quad (1)$$

where  $\psi(\vec{r}, t)$  is the relevant order parameter at point  $\vec{r}$  and time  $t$ . The angular brackets in Eq. (1) refer to an averaging over independent initial conditions and noise realizations; and  $g(x)$  is a scaling function, which is independent of time. This dynamical-scaling property reflects the fact that the morphology of the coarsening system is statistically self-similar in time, and only changes by a scale factor. Experimental studies usually measure the time-dependent structure factor  $S(\vec{k}, t)$ , which is the Fourier transform of  $C(\vec{r}, t)$  at wave vector  $\vec{k}$ . The appropriate dynamical-scaling property for the structure factor is  $S(\vec{k}, t) = L(t)^d f(kL(t))$ , where  $d$  is the dimensionality; and the scaling function  $f(y)$  is also independent of time.

Most studies of phase separation have focused upon determining the behavior of  $L(t)$  and the scaling functions  $g(x)$  or  $f(y)$  [1]. In the case of binary mixtures without hydrodynamic effects, there is a reasonable understanding of domain growth, which is driven by the evaporation-condensation mechanism. The resultant growth law is the so-called Lifshitz-Slyozov (LS) law,  $L(t) \sim t^{1/3}$  [3]. The scaling form of the structure factor  $f(y)$  has also been the subject

of intense study and has been characterized both experimentally and numerically [1]. Our analytical understanding of the structure factor is not yet complete, and is confined to the limit where one of the components is present in a vanishingly small fraction [3]. For the important case of a critical quench, i.e., approximately equal fractions of both components, there is an analytical understanding of  $f(y)$  for  $y \rightarrow 0$  and  $y \rightarrow \infty$  [1]. However, there is no comprehensive theory which interpolates between these two extremes.

Recent studies have attempted to incorporate and understand the effects of various experimentally relevant features on the dynamics of phase separation, e.g., quenched and annealed disorders [4]; surfaces with a preferential attraction for one of the components of the binary mixture [5]; systematic flow fields; etc. An important class of studies in this context has investigated phase separation in polymer-solvent mixtures, with particular focus upon polymer-specific properties. Our present study belongs to this class – we investigate domain growth in polymer-solvent mixtures, where the polymer-rich region undergoes gelation. In particular, we are interested in the impact of reduced mobility of the gel phase on the kinetics and morphology of phase separation.

This paper is organized as follows. Section II summarizes available numerical and analytical results for this problem. Section III describes our dynamical model and its linear stability analysis. In Section IV, we present detailed numerical results obtained from simulations of the dynamical model. Finally, Sec. V concludes this paper with a summary and discussion of our results.

### II. SUMMARY OF AVAILABLE NUMERICAL AND ANALYTICAL RESULTS

In this section, we undertake a brief review of available numerical and analytical results for phase-separating polymer-solvent mixtures when the polymer undergoes gelation. There have also been many experimental studies of the interplay of phase separation and gelation. It is not our intention to review these here, but we discuss representative results which will motivate our subsequent discussion. The process of gelation corresponds to the formation of an interconnected (or percolated) structure due to chemical bonding or topological crosslinkages. Experimentalists differentiate

between: (a) chemical or irreversible gels, where the crosslinking is due to strong covalent bonds; and (b) physical or reversible gels, where the crosslinking is due to weak hydrogen bonds or topological constraints. In a mean-field (MF) approach, the gelation condition is  $\phi^2[e^{\beta_g K}/(1 + e^{\beta_g K})] = p_c$ , where  $\phi$  is the polymer density;  $K$  is the bond strength;  $\beta_g = 1/T_g$ , where  $T_g$  is the gelation temperature ( $k_B = 1$ ); and  $p_c$  is the percolation probability. In general, viscosity in gels is extremely high and the diffusive transport of particles through a gel is strongly suppressed.

Next, we consider a polymer-solvent mixture which has been quenched below the miscibility gap. This mixture rapidly segregates into polymer-rich and solvent-rich regions. The polymer-rich regions can undergo gelation depending on the temperature  $T$ , and local polymer density  $\phi$ . If  $T > T_g(\phi)$ , the phase-separation process proceeds to completion. If  $T < T_g(\phi)$ , the relative time scales of segregation ( $\tau_s$ ) and gelation ( $\tau_g$ ) are critical. When  $\tau_s \ll \tau_g$ , the phase-separation process again proceeds to completion. However, if  $\tau_s \geq \tau_g$ , there is an interesting interplay of phase separation and gelation. In this case, the gel formation can drastically slow down (or even freeze) phase separation because of the suppression of diffusion [6]. This is the situation we will focus upon in the present paper. Similar physical situations arise in the context of systems with chemical crosslinking reactions [7]; and photo crosslinking [8].

Before we proceed, it is relevant to briefly mention some related studies involving polymer blends (AB) with crosslinking between the polymers A and B. These systems are referred to as “interpenetrated networks” (IPN’s) and are of considerable technological importance [9]. The static aspects of these systems have been discussed by de Gennes [10]; and analytic studies of early-time kinetics subsequent to a quench are due to Derouiche *et al.* [11], and Chikina and Daoud [12]. An experimental study (via small-angle neutron scattering) of microphase separation in IPN was done by Brulet *et al.* [13].

Let us now return to phase separation in polymer-solvent mixtures. Numerical studies have attempted to model and replicate the experimental behavior discussed above. One class of studies models the gel formation by introducing an order-parameter-dependent mobility in the continuity equation for the local composition variable. This mobility is set to zero (or nearly zero) in the gel phase. An early study in this class is due to Sciortino *et al.* [14], who numerically investigated two-dimensional phase separation in a polymer-solvent mixture at critical composition, i.e., with equal fractions of both components. These authors found that the coarsening system rapidly froze into a microstructure, and they studied the onset of freezing and the morphology of the microstructure. Sappelt and Jackle [15] have also investigated similar models in  $d = 2$ , though in the (equivalent) context of a glass-forming phase. These authors undertook a detailed numerical study of a wide range of mixture compositions, and distinguished between two physical situations. In the case where the “gel” (or glass) phase is the minority phase, domain growth proceeds unhindered because there is a connected region of high mobility for transport of polymer molecules. The corresponding domain growth law is the

usual LS law,  $L(t) \sim t^{1/3}$ . In the case where the “gel” (or glass) phase is the majority phase, domain growth is hindered by the presence of a percolated low-mobility phase. However, Sappelt and Jackle did not observe complete freezing in their simulations—rather, they found that domain growth proceeds (albeit slowly) through the collective motion of droplets of the minority phase.

The model we investigate in this paper also belongs to the above class. However, the focus of our study is different. Both of the above studies are deterministic, and do not include thermal fluctuations. On the other hand, we are particularly interested in the effects of thermal fluctuations on domain growth in these systems.

An alternative approach to this problem was formulated by Sekimoto *et al.* [16], who investigated a  $d = 2$  microscopic model for a polymer-solvent mixture, which explicitly accounted for the elastic energy associated with gel deformations. These authors demonstrated that the coarsening system froze into a sponge-like structure, consisting of polymer-rich and solvent-rich domains, as a result of elastic pinning. Onuki and Puri [17] have used similar considerations to formulate a dynamical model with a suitable coarse-grained free-energy functional [18]. They studied this model numerically for  $d = 2$  and observed slow coarsening of the system in a sponge-like domain structure. Onuki and Puri also used their model to obtain domain morphologies for the uniaxial case, where domains are oriented in a particular direction. Again, both of these studies neglected the effects of thermal fluctuations.

Finally, we discuss a Monte Carlo (MC) study by Glotzer *et al.* [19]. These authors considered a monomer-solvent mixture on a lattice, with nearest-neighbor monomers being allowed to interact with two highly different energies—corresponding to the absence or presence of a chemical bond [20]. Glotzer *et al.* investigated phase-separation dynamics in this model using the standard Kawasaki spin-exchange kinetics. Their results showed that the initial stage of domain growth (when there are few chemical bonds) is analogous to that for simple binary mixtures. However, a sufficiently large fraction of strong bonds gives rise to a pinning effect, which effectively freezes the evolving system into a microstructure. Of course, this system would ultimately coarsen into a two-domain equilibrium structure but the time scales become extremely long. However, as Glotzer *et al.* remark, “freezing” in their MC model is a consequence of the fact that the microscopic spin-exchange kinetics is only permitted to move one spin at a time—in this sense, the MC results are of restricted relevance for real experiments.

### III. DYNAMICAL MODEL AND LINEAR STABILITY ANALYSIS

#### A. Lattice model and coarse-grained free energy

The starting point of our modeling is the lattice model of Glotzer *et al.* [19]. We consider a monomer-solvent (A-B) mixture on a cubic lattice with the Hamiltonian

$$H = -\epsilon_{AA} \sum_{\langle ij \rangle} n_i^A n_j^A - \epsilon_{BB} \sum_{\langle ij \rangle} n_i^B n_j^B + \epsilon_{AB} \sum_{\langle ij \rangle} (n_i^A n_j^B + n_i^B n_j^A) - K \sum_{\langle ij \rangle} \tau_{ij} n_i^A n_j^A, \quad (2)$$

where  $\epsilon_{IJ} (>0)$  refers to the nearest-neighbor interaction energy between species  $I$  and  $J$ ; and  $n_i^A, n_i^B$  are the occupation-number variables at site  $i$  for species  $A$  and  $B$ , respectively. In Eq. (2), we have introduced the additional bond variable  $\tau_{ij} \in \{0,1\}$ , which gives rise to an additional energy ( $-K$ ) if a chemical bond exists between two monomers. For a configuration with  $n_l^A = n_m^A = 0$ , we always have  $\tau_{lm} = 0$ . It is straightforward to demonstrate that  $\langle \tau_{lm} \rangle = e^{\beta K} / (1 + e^{\beta K})$  for a configuration with  $n_l^A = n_m^A = 1$ , where  $\beta = 1/T (k_B = 1)$ .

Without loss of generality, we set  $\epsilon_{AA} = \epsilon_{BB} = \epsilon_{AB} = \epsilon$ . Recalling that  $n_i^B = 1 - n_i^A$ , we obtain

$$H = - \sum_{\langle ij \rangle} (4\epsilon + K\tau_{ij}) n_i n_j, \quad (3)$$

where we have dropped constant terms, and simplified notation ( $n_i^A \equiv n_i$ ). The appropriate ensemble has fixed  $T$ , composition, and number of sites  $N$ . It is straightforward to sum over the bond variables [19] to obtain the partition function

$$Z = \sum'_{\{n_i\}} \exp \left\{ [4\beta\epsilon + \ln(1 + e^{\beta K})] \sum_{\langle ij \rangle} n_i n_j \right\} \equiv \sum'_{\{n_i\}} \exp \{-\beta H_{\text{eff}}\}, \quad (4)$$

where the sum over configurations  $\{n_i\}$  is constrained by the overall composition of the binary mixture. Thus, our problem reduces to the usual lattice gas (or Ising model), for which many exact results are available.

Subsequently, we will consider the dynamical evolution of a coarse-grained (mean-field or MF) version of this Hamiltonian. In MF theory, the critical coexistence temperature  $T_c$  is defined through ( $\beta_c = 1/T_c$ )

$$\frac{q}{4} [4\beta_c \epsilon + \ln(1 + e^{\beta_c K})] = 1, \quad (5)$$

where  $q$  is the coordination number of the lattice. The monomer densities in the coexisting phases are  $\phi_0 = (1 \pm \psi_0)/2$ , where  $\psi_0$  is the positive solution of the transcendental equation

$$\psi_0 = \tanh \left\{ \frac{q}{4} [4\beta_c \epsilon + \ln(1 + e^{\beta_c K})] \psi_0 \right\}. \quad (6)$$

Next, let us consider the coarse-grained version of the above lattice model, obtained using the Bragg-Williams approximation. First, we consider the Helmholtz free energy per spin for a homogeneous configuration with  $\langle n_i \rangle = \phi$ ,  $\langle \tau_{ij} \rangle = \theta$ , viz.,

$$f(\phi, \theta) \simeq -\frac{q}{2} (4\epsilon + K\theta) \phi^2 + T[\phi \ln \phi + (1 - \phi) \ln(1 - \phi)] + \frac{qT}{2} \phi^2 [\theta \ln \theta + (1 - \theta) \ln(1 - \theta)], \quad (7)$$

where there are two entropy terms: one for the site-occupation variables and the other for the bond-occupation variables. For order-parameter fields which vary slowly in space, we generalize the above expression to obtain

$$F[\phi, \theta] = \int \vec{d}r \left[ f(\phi, \theta) + \frac{\sigma}{2} (\vec{\nabla} \phi)^2 \right], \quad (8)$$

where we have introduced surface tension at the monomer-solvent boundary with strength  $\sigma$ .

### B. Dynamical model and linear stability analysis

The density field is conserved and we associate dissipative ‘‘model B’’ dynamics with it [21]. In the absence of thermal fluctuations, the appropriate evolution equation is

$$\begin{aligned} \frac{\partial \phi(\vec{r}, t)}{\partial t} &= -\vec{\nabla} \cdot \vec{J}(\vec{r}, t) = -\vec{\nabla} \cdot \left\{ M(\phi, \theta) \vec{\nabla} \left[ \frac{\delta F}{\delta \phi} \right] \right\} \\ &= \vec{\nabla} \cdot \left\{ M(\phi, \theta) \vec{\nabla} \left[ -q(4\epsilon + K\theta) \phi + T \ln \left( \frac{\phi}{1 - \phi} \right) \right. \right. \\ &\quad \left. \left. + qT \phi [\theta \ln \theta + (1 - \theta) \ln(1 - \theta)] - \sigma \nabla^2 \phi \right] \right\}. \end{aligned} \quad (9)$$

In Eq. (9), the current  $\vec{J}(\vec{r}, t)$  is proportional to the gradient of the chemical potential. We have explicitly introduced an order-parameter-dependent mobility  $M(\phi, \theta)$ , which has a strong dependence on whether or not the system is locally in the gel phase. The precise form of this function will be discussed later. The time scale of phase separation ( $\tau_s$ ) is also incorporated in  $M(\phi, \theta)$ .

The chemical bonding which results in gel formation also has an associated dynamics, which we model as a relaxational nonconserved (‘‘model A’’) dynamics [21] as follows:

$$\frac{\partial \theta(\vec{r}, t)}{\partial t} = -\bar{M} \frac{\delta F}{\delta \theta} = \frac{q\bar{M}}{2} \phi^2 \left[ K - T \ln \left( \frac{\theta}{1 - \theta} \right) \right]. \quad (10)$$

In Eq. (10), the constant mobility  $\bar{M}$  incorporates the time scale of gelation  $\tau_g$ . This equation has the static fixed point  $\theta_s = e^{\beta K} / (1 + e^{\beta K})$ , as expected. Furthermore, the time scale of relaxation to this fixed point depends upon the local monomer density—there can be no chemical bonds in regions where there are no monomers.

The system is initially in a high-temperature homogeneous phase with  $\phi(\vec{r}, t) = \phi_0 + \xi(\vec{r}, t)$ ;  $\theta(\vec{r}, t) = \bar{\theta}(t) + \chi(\vec{r}, t)$  ( $\bar{\theta}(0) = \theta_0$ ), where the fields  $\xi(\vec{r}, t)$  and  $\chi(\vec{r}, t)$  are small-amplitude fluctuations. We have introduced a systematic time-dependent solution,  $\bar{\theta}(t) = V^{-1} \int \vec{d}\vec{r} \theta(\vec{r}, t)$ , for rea-

sons which will shortly become clear. Subsequent to the quench, the growth of these fluctuations is determined by the appropriate linearized equations

$$\begin{aligned} \frac{\partial \xi(\vec{r}, t)}{\partial t} = M(\phi_0, \bar{\theta}) \nabla^2 \left\{ \left[ -q[4\epsilon + K\bar{\theta} - T\bar{\theta} \ln \bar{\theta} \right. \right. \\ \left. \left. - T(1 - \bar{\theta}) \ln(1 - \bar{\theta}) \right] + \frac{T}{\phi_0(1 - \phi_0)} \right\} \xi \\ - q\phi_0 \left[ K - T \ln \left( \frac{\bar{\theta}}{1 - \bar{\theta}} \right) \right] \chi - \sigma \nabla^2 \xi \}, \quad (11) \end{aligned}$$

and

$$\begin{aligned} \frac{d\bar{\theta}(t)}{dt} + \frac{\partial \chi(\vec{r}, t)}{\partial t} = \frac{q\bar{M}}{2} \phi_0^2 \left[ K - T \ln \left( \frac{\bar{\theta}}{1 - \bar{\theta}} \right) \right] \\ + q\bar{M} \phi_0 \left[ K - T \ln \left( \frac{\bar{\theta}}{1 - \bar{\theta}} \right) \right] \xi \\ - \frac{q\bar{M}}{2} \frac{T\phi_0^2}{\bar{\theta}(1 - \bar{\theta})} \chi. \quad (12) \end{aligned}$$

The inhomogeneous term on the right-hand-side of Eq. (12) determines the thermalization of  $\bar{\theta}(t)$  to its equilibrium value

$$\bar{\theta}(\infty) = \theta_s = \frac{e^{\beta K}}{1 + e^{\beta K}}. \quad (13)$$

More generally, we consider the Fourier transform of Eqs. (11)–(12) without the systematic piece as follows:

$$\begin{aligned} \frac{\partial \xi(\vec{k}, t)}{\partial t} = M(\phi_0, \bar{\theta}) k^2 \left\{ \left[ q[4\epsilon + K\bar{\theta} - T\bar{\theta} \ln \bar{\theta} \right. \right. \\ \left. \left. - T(1 - \bar{\theta}) \ln(1 - \bar{\theta}) \right] - \frac{T}{\phi_0(1 - \phi_0)} - \sigma k^2 \right\} \xi \\ + q\phi_0 \left[ K - T \ln \left( \frac{\bar{\theta}}{1 - \bar{\theta}} \right) \right] \chi \} \\ \equiv a_{11} \xi(\vec{k}, t) + a_{12} \chi(\vec{k}, t), \quad (14) \end{aligned}$$

and

$$\begin{aligned} \frac{\partial \chi(\vec{k}, t)}{\partial t} = q\bar{M} \phi_0 \left[ K - T \ln \left( \frac{\bar{\theta}}{1 - \bar{\theta}} \right) \right] \xi - \frac{q\bar{M}}{2} \frac{T\phi_0^2}{\bar{\theta}(1 - \bar{\theta})} \chi \\ \equiv a_{21} \xi(\vec{k}, t) + a_{22} \chi(\vec{k}, t). \quad (15) \end{aligned}$$

We can obtain a general solution of this matrix equation, even though the coefficients  $a_{ij}$  are time dependent. However, recall that  $\bar{\theta}(t)$  is exponentially saturated to its equilib-

rium value. Therefore, we consider the dynamics of fluctuations with  $\bar{\theta}(t) = \theta_s$ . This simplifies Eqs. (14)–(15) as follows:

$$\begin{aligned} \frac{\partial \xi(\vec{k}, t)}{\partial t} = M(\phi_0, \theta_s) k^2 \left\{ q[4\epsilon + T \ln(1 + e^{\beta K})] \right. \\ \left. - \frac{T}{\phi_0(1 - \phi_0)} - \sigma k^2 \right\} \xi \\ \equiv \lambda_\xi(\vec{k}) \xi(\vec{k}, t), \quad (16) \end{aligned}$$

$$\frac{\partial \chi(\vec{k}, t)}{\partial t} = -\frac{q\bar{M}}{2} \frac{T\phi_0^2}{\theta_s(1 - \theta_s)} \chi \equiv \lambda_\chi \chi(\vec{k}, t). \quad (17)$$

These equations have the obvious solutions  $\xi(\vec{k}, t) = \exp[\lambda_\xi(\vec{k})t] \xi(\vec{k}, 0)$ ;  $\chi(\vec{k}, t) = \exp[\lambda_\chi t] \chi(\vec{k}, 0)$ , fixing the time scales of growth and decay of initial fluctuations in terms of parameters, which can be experimentally obtained. As expected from the static considerations of Sec. III A, the instability condition is

$$q[4\beta\epsilon + \ln(1 + e^{\beta K})] - \frac{1}{\phi_0(1 - \phi_0)} > 0. \quad (18)$$

If the system is unstable to phase separation, the growth of initial fluctuations is amplified by the presence of chemical bonds. This is because the system finds it both energetically and entropically favorable to phase separate into polymer-rich regions, thereby facilitating the formation of chemical bonds.

### C. Incorporation of thermal noise and dimensionless rescaling

We will consider the physically relevant limit where the time scale of gelation ( $\tau_g$ ) is much faster than the time scale of segregation ( $\tau_s$ ). Thus, the bond variable  $\theta(\vec{r}, t) = \theta_s$  everywhere and the appropriate dynamical equation for  $\phi(\vec{r}, t)$  is

$$\begin{aligned} \frac{\partial \phi(\vec{r}, t)}{\partial t} = \vec{\nabla} \cdot \left\{ M(\phi, \theta_s) \vec{\nabla} \left[ -q[4\epsilon + T \ln(1 + e^{\beta K})] \phi \right. \right. \\ \left. \left. + T \ln \left( \frac{\phi}{1 - \phi} \right) - \sigma \nabla^2 \phi \right] \right\} \\ \equiv -\vec{\nabla} \cdot \vec{J}(\vec{r}, t), \quad (19) \end{aligned}$$

which is just the usual Cahn-Hilliard (CH) equation with an order-parameter-dependent mobility. We introduce thermal fluctuations through a conserved noise term in the current as

$$\frac{\partial \phi(\vec{r}, t)}{\partial t} = -\vec{\nabla} \cdot \{ \vec{J}(\vec{r}, t) + \vec{\eta}(\vec{r}, t) \}. \quad (20)$$

For the case of constant mobility,  $M(\phi, \theta_s) = M_0$ , there is a standard prescription for the properties of noise so that the

system approaches its correct equilibrium, i.e., the Gaussian white noise has a zero average and obeys the fluctuation-dissipation relation

$$\begin{aligned} \langle \vec{\eta}(\vec{r}, t) \rangle &= 0, \\ \langle \eta_i(\vec{r}, t) \eta_j(\vec{r}', t') \rangle &= 2M_0 T \delta_{ij} \delta(\vec{r} - \vec{r}') \delta(t - t'). \end{aligned} \quad (21)$$

In the present context, we are interested in a physical situation where the mobility explicitly depends upon the order parameter, i.e., we expect the mobility to be drastically diminished in the gel phase. To the best of our knowledge, there is no clear prescription for the correct properties of noise in this case. The straightforward generalization replaces  $M_0$  in Eq. (21) by the corresponding order-parameter-dependent mobility [22]. There is some justification for such a generalization. For example, Dean [23] has derived the stochastic equation obeyed by the density variable in an assembly of Brownian particles interacting through a pair potential. This stochastic equation involves an order-parameter-dependent mobility of the form  $M(\phi) = M_0 \phi$ , and Dean demonstrates the above generalization to be correct in this context. More generally, the above prescription is only the first term in a Taylor-series expansion [24]. In the present paper, we model thermal fluctuations by replacing  $M_0 \rightarrow M(\phi, \theta_s)$  in Eq. (21). We should stress that we are interested in the far-from-equilibrium evolution of the system, rather than the final approach to equilibrium, which would depend more sensitively on the precise nature of thermal fluctuations.

Next, we model the mobility following Sciortino *et al.* [14], and Sappelt and Jackle [15]. Recall that the mobility is very low in the gel-rich phase and normal in the solvent-rich phase. The density of chemical bonds in a region is  $p = \phi^2 \theta_s$ , and the region is in the gel phase if  $p > p_c$ , the corresponding percolation probability. Therefore, we set  $M(\phi, \theta_s) = M_0 h(\phi) \equiv M_0 \tilde{h}(p_c - \phi^2 \theta_s)$ , where  $\tilde{h}(x) = 0$  if  $x \leq 0$  and  $\tilde{h}(x) = 1$  if  $x > 0$ .

For the simulations described in Sec. IV, it is convenient to introduce the order parameter  $\psi = 2\phi - 1$ . The corresponding dynamical equation for the order parameter is

$$\begin{aligned} \frac{\partial \psi(\vec{r}, t)}{\partial t} &= \vec{\nabla} \cdot \left\{ M(\psi, \theta_s) \vec{\nabla} \left[ 4T - 4q\epsilon - qT \ln(1 + e^{\beta K}) \right] \psi \right. \\ &\quad \left. + \frac{4T}{3} \psi^3 - \sigma \nabla^2 \psi \right\} + \vec{\eta}, \end{aligned} \quad (22)$$

where we have expanded the function  $g(\psi) = \ln(1 + \psi) - \ln(1 - \psi)$  up to cubic order in  $\psi$ . The mobility is now defined as

$$M(\psi, \theta_s) = M_0 h(\psi) \equiv M_0 \tilde{h} \left[ p_c - \left( 1 + \frac{\psi}{\psi_s} \right)^2 \frac{\theta_s}{4} \right],$$

where  $\psi_s$  is the saturation value of the order parameter.

Finally, we introduce dimensionless rescaling as follows (with  $T < T_c$ ):

$$\begin{aligned} \psi &= \psi_s \psi', \quad \psi_s = \sqrt{3 \left[ q\beta\epsilon + \frac{q}{4} \ln(1 + e^{\beta K}) - 1 \right]}; \\ \vec{r} &= \xi \vec{r}', \quad \xi = \sqrt{\frac{\sigma}{4T \left[ q\beta\epsilon + \frac{q}{4} \ln(1 + e^{\beta K}) - 1 \right]}}; \\ t &= \tau t', \quad \tau = \frac{3\xi^2}{4TM_0\psi_s^2}; \\ \vec{\eta} &= \frac{2TM_0\psi_s^3}{3\xi} \vec{\eta}'. \end{aligned} \quad (23)$$

This results in the dimensionless equation (dropping primes) are

$$\frac{\partial \psi(\vec{r}, t)}{\partial t} = \vec{\nabla} \cdot \{ h(\psi) \vec{\nabla} [-\psi + \psi^3 - \nabla^2 \psi] + \vec{\eta} \}, \quad (24)$$

with

$$\begin{aligned} \langle \vec{\eta}(\vec{r}, t) \rangle &= 0, \\ \langle \eta_i(\vec{r}, t) \eta_j(\vec{r}', t') \rangle &= \frac{6}{\psi_s^{4-d}} \left( \frac{4T}{3\sigma} \right)^{d/2} h(\psi) \delta_{ij} \delta(\vec{r} - \vec{r}') \delta(t - t') \\ &\equiv \epsilon h(\psi) \delta_{ij} \delta(\vec{r} - \vec{r}') \delta(t - t'), \end{aligned} \quad (25)$$

where  $\epsilon$  measures the strength of ‘‘dimensionless’’ noise; and  $h(\psi) \equiv \tilde{h}[p_c - (1 + \psi)^2(\theta_s/4)]$ . This is the model we use to obtain the numerical results which are presented in the next Sec. IV.

#### IV. DETAILED NUMERICAL RESULTS

We have numerically solved Eqs. (24)–(25) on a  $d=2$  lattice of size  $N^2$ , with periodic boundary conditions in both directions. We used an isotropic Euler-discretization scheme to approximate derivatives. The discretization mesh sizes were  $\Delta x = 1.3$  and  $\Delta t = 0.05$ . We work in the strong-bonding limit with  $K$  large so that  $\theta_s \approx 1$ . The initial condition for the order-parameter field  $\psi(\vec{r}, 0)$  in each run consisted of uniformly distributed small-amplitude fluctuations about an average value  $\psi_0$ . Thermal noise of amplitude  $\epsilon$  was mimicked by uniformly distributed random numbers with amplitude  $A = \sqrt{3\epsilon/\Delta x^d \Delta t}$ . We have also performed simulations with Gaussian-distributed noise and the results are similar to those presented here for uniformly distributed noise.

We characterize domain growth from a homogeneous initial condition by: (a) evolution pictures and profiles; (b) time-dependent structure factors; and (c) characteristic length scales. The structure factor is defined as  $S(\vec{k}, t) = \langle |\bar{\psi}(\vec{k}, t)|^2 \rangle$ , where  $\bar{\psi}(\vec{k}, t)$  is the discrete Fourier transform of  $\bar{\psi}(\vec{r}, t) = \psi(\vec{r}, t) - \psi_0$ , and the angular brackets refer to an averaging over different initial conditions and noise realizations. For a  $d=2$  lattice, the wave vectors take discrete val-

ues  $\vec{k} = (2\pi/N\Delta x)(n_x, n_y)$ , where  $n_x$  and  $n_y$  range from  $-(N/2)$  to  $(N/2) - 1$ . The structure factors are normalized as  $N^{-2} \sum_{\vec{k}} S(\vec{k}, t) = 1$ , and then spherically averaged to obtain the scalar function  $S(k, t)$ . The structure-factor data presented here are obtained as an average over 20 independent runs for systems of size  $N=512$ . The characteristic length scale  $L(t)$  is defined as the inverse of the first moment of the scalar structure factor, i.e.,  $L(t) = \langle k \rangle^{-1}$ , where

$$\langle k \rangle = \frac{\int_0^{k_m} dk k S(k, t)}{\int_0^{k_m} dk S(k, t)}. \quad (26)$$

In Eq. (26),  $k_m$  is the upper cutoff on the discrete lattice value of  $k$ . Typically, we set  $k_m$  equal to half the magnitude of the largest wave vector lying in the Brillouin zone of the lattice.

### A. Results for case with $T=0$

Let us first focus on results from deterministic simulations, with  $\epsilon=0$  ( $T=0$ ) in Eqs. (24)–(25). These results are analogous to those obtained earlier by Sciortino *et al.* [14]; and Sappelt and Jackle [15].

Figure 1 shows the temporal evolution resulting from a random initial condition with  $\psi_0=0.3$ . All evolution pictures presented in this paper were obtained for lattices of size  $N=256$ . Regions with order parameter  $\psi > 0$  (polymer-rich) are marked in black, and regions with  $\psi < 0$  (solvent-rich) are unmarked. Recall that the gel phase is defined as a region where a percolated cluster has formed, i.e.,  $\phi^2 \theta_s \geq \phi_g^2 \theta_s = 1/2$  for  $d=2$ . For  $\theta_s \approx 1$ , we have  $\phi_g \approx 0.71$  and  $\psi_g \approx 0.41$ . Thus, the dynamical evolution is frozen in regions with  $\psi \geq \psi_g$ . Because of the asymmetry in local values of the order parameter, the fractions of the gel and solvent phases are  $f_g = (1 + \psi_0)/(1 + \psi_g)$  and  $f_s = (\psi_g - \psi_0)/(1 + \psi_g)$ , respectively. Therefore, the gel phase percolates the lattice for  $\psi_0 > (\psi_g - 1)/2$ . Figure 1 shows the emergence of droplets of the solvent-rich phase in a percolated matrix of zero-mobility gel phase. As expected, the system “freezes” into a microstructure, though there may still be an extremely slow growth due to cooperative motion of droplets [15]. Figure 2 shows the order-parameter profiles corresponding to the evolution pictures in Fig. 1. It is clear from these profiles that the dynamical evolution is frozen in most regions of the system.

Figure 3 demonstrates the dynamical scaling of the time-dependent structure factor for the evolution shown in Fig. 1. In this figure, we superpose data for  $S(k, t)L(t)^{-2}$  versus  $kL(t)$  from different times. The scaling is excellent, which is an obvious consequence of the fact that there is almost no evolution of the morphology!! Nevertheless, the form of the scaling function is of interest to us. We will subsequently compare this function with the scaling function for the case with thermal noise.

Figure 4(a) plots the characteristic length scale  $L(t)$  versus  $t$  for a range of values of  $\psi_0$ . Our simple argument above

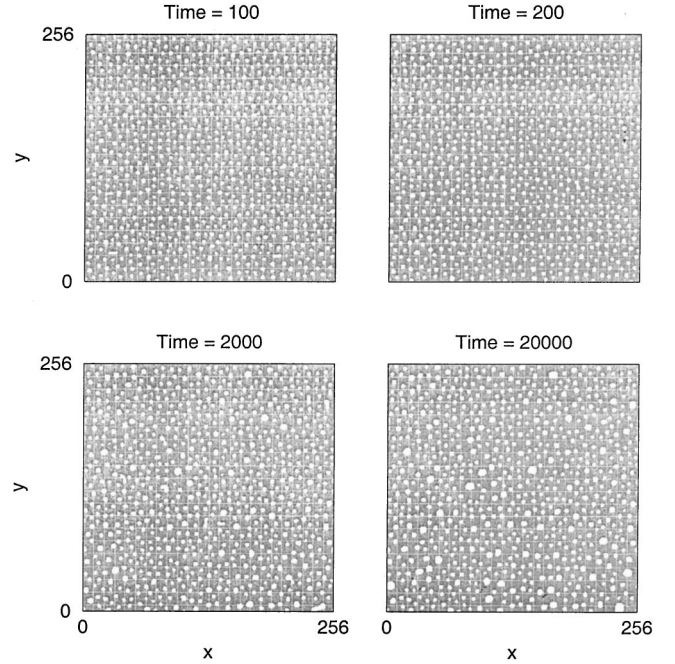


FIG. 1. Temporal evolution of our model from a random initial condition. The initial state consisted of an order-parameter field with uniformly distributed small-amplitude fluctuations about an average value  $\psi_0=0.3$ . The evolution pictures are obtained from an isotropic Euler discretization of the deterministic version of Eqs. (24)–(25) ( $\epsilon=0$ ) with mesh sizes  $\Delta x=1.3$  and  $\Delta t=0.05$ . The discrete equations were implemented on a  $d=2$  lattice of size  $N^2$ , with periodic boundary conditions in both directions. The snapshots shown correspond to the case with  $N=256$ . Regions with order parameter  $\psi > 0$  (polymer rich) are marked in black, while regions with  $\psi < 0$  (solvent rich) are unmarked. The evolution times labeling each snapshot refer to the time after the initial quench.

suggests that the polymer-rich phase is a majority phase for  $\psi_0 \geq -0.29$ . However, numerical results show that the value of  $\psi_0$  at which both phases percolate is  $\psi_0 \approx -0.2$ . For  $\psi_0 \leq -0.2$ , the high-mobility phase percolates and there is no hindrance of the usual evaporation-condensation mechanism for phase separation [1]. In this case, the numerical data for the length scale is consistent with the LS growth law,  $L(t) \sim t^{1/3}$ . For  $\psi_0 \geq -0.2$ , the phase-separation process is “frozen” due to the absence of diffusion in the percolated zero-mobility region. For  $\psi_0 > -0.2$ , cooperative growth modes contribute and a slow dynamical evolution is seen. This is a consequence of collective motion of solvent droplets in the gel phase—driven by chemical potential gradients [15]. Figure 4(b) replots the data from Fig. 4(a) on a log-log scale.

### B. Results for case with $T>0$

As we have stated earlier, our primary interest in this paper is the effect of thermal fluctuations on the above scenario. The introduction of noise in the context of a system with order-parameter-dependent mobility has already been discussed in Sec. III C. We have obtained numerical results for a range of moderate values of the noise amplitude, and these results are similar up to prefactors. In this paper, we present representative numerical results for  $\epsilon=0.1$ .

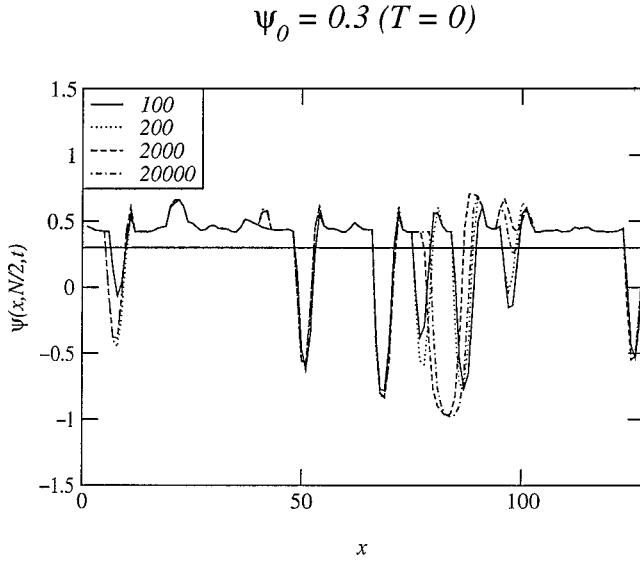


FIG. 2. Order-parameter profiles for the evolution pictures in Fig. 1. We plot the order parameter  $\psi(x, N/2, t)$  vs  $x$  along a horizontal cross section at the middle of the lattice. For clarity, we only present profiles for the region  $x \in [0, N/2]$ . The profiles are shown for  $t = 100, 200, 2000, 20000$ , and are denoted by the specified line types. For reference, a horizontal line is drawn at  $\psi_0 = 0.3$ .

Figure 5 shows the temporal evolution in the noisy case from a homogeneous initial condition with  $\psi_0 = 0.3$ . Figure 5 should be contrasted with Fig. 1—there are no signs of “freezing” or slow growth in the present context. The zero-mobility phase still percolates the system, so domain growth cannot occur via the evaporation-condensation mechanism. However, the thermal noise induces Brownian motion of droplets and phase separation proceeds via a droplet coalescence mechanism. Figure 6 shows the order-parameter profiles corresponding to the evolution pictures in Fig. 5.

Next, we examine the scaling of the time-dependent structure factor. Figure 7 plots data for  $S(k, t)L(t)^{-2}$  versus  $kL(t)$  from different times. Again, the scaling is excellent, though the system undergoes rapid evolution in this case. The solid line refers to the scaled structure factor (at  $t = 20000$ ) from the deterministic case shown in Fig. 3. The difference in the scaled structure factors for the deterministic and noisy cases reflects the difference in the morphologies. For the  $T = 0$  case, the initial fluctuations become trapped and well-formed domains are largely absent. The  $T = 0$  morphology (see Fig. 1) is comparable to the initial stages of growth for the  $T > 0$  case, e.g., compare pictures at  $t = 20000$  in Fig. 1 and  $t = 100$  in Fig. 5. Figure 7(b) is a log-log plot of the scaled structure factor data. The straight line with slope  $-3$  corresponds to the  $d = 2$  Porod law,  $S(k, t) \sim k^{-(d+1)}$  for large  $k$ , which characterizes scattering off sharp interfaces. Our numerical data for the  $T > 0$  case is in conformity with the Porod law, indicating the presence of sharp domain walls.

Finally, we investigate the time dependence of the characteristic length scale in Fig. 8, which plots  $\ln[L(t)]$  versus  $\ln t$  for  $\psi_0 = 0.4, 0.3, 0.2$  (upper frame) and  $\psi_0 = 0.0, -0.2, -0.3, -0.4$  (lower frame). The numerical results in the upper frame demonstrate that Brownian motion of droplets (driven

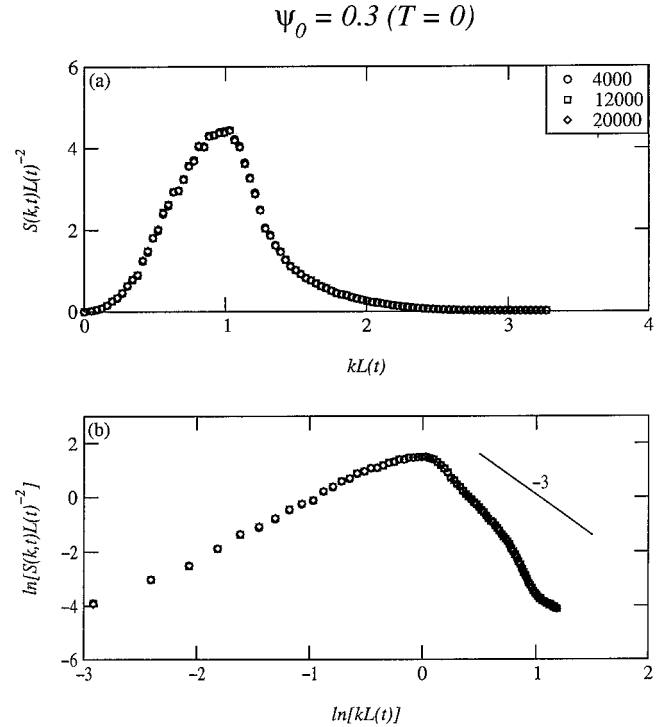


FIG. 3. (a) Superposition of data for  $S(k, t)L(t)^{-2}$  vs  $kL(t)$  from times  $t = 4000, 12000, 20000$ —denoted by the specified symbols. The simulation details and parameters are the same as in Fig. 1. The structure-factor data are obtained as an average over 20 independent runs for lattices of size  $N = 512$ . The length scale  $L(t)$  is defined as the reciprocal of the first moment of the spherically averaged structure factor. (b) Plot of  $\ln[S(k, t)L(t)^{-2}]$  vs  $\ln[kL(t)]$  for data from (a). The solid line has a slope of  $-3$  and refers to Porod’s law,  $S(k, t) \sim k^{-(d+1)}$  for large  $k$ , which characterizes scattering off sharp interfaces [1].

by thermal fluctuations) restores a LS-like growth law  $L(t) \sim t^{1/3}$ . This is the central result of the present paper. There are no signs of freezing in this case, unlike in the deterministic case, and domain growth apparently proceeds to completion. Of course, although the growth law is similar to the LS law, the mechanism involved is quite different. Domain growth occurs via the Brownian motion and coalescence of droplets. Consider a droplet of size  $L$ . The diffusion constant of this droplet is  $D \sim T/L$ , and the time  $t$  required to traverse a distance  $L$  scales as  $L^2 \sim (T/L)t$ . Thus, we expect  $L(t) \sim (Tt)^{1/3}$  for domain growth by Brownian coalescence. The argument is analogous to that of Ohta [25]; and Siggia [26] in the context of binary fluids. The numerical results in the lower frame are also consistent with the LS growth law, although the data for  $\psi_0 = 0.0$  is still not in the asymptotic regime. For  $\psi_0 < -0.2$ , domain growth occurs due to both evaporation-condensation and Brownian coalescence mechanisms, which give rise to identical growth laws.

Experimentalists [6] have emphasized that phase separating polymer-solvent systems freeze into microstructures only when the quenches are deep. Bansil *et al.* [6] have argued that this is because the time scales of phase separation and gelation are comparable only at low temperatures, allowing the gelation process to interfere with the phase-separation

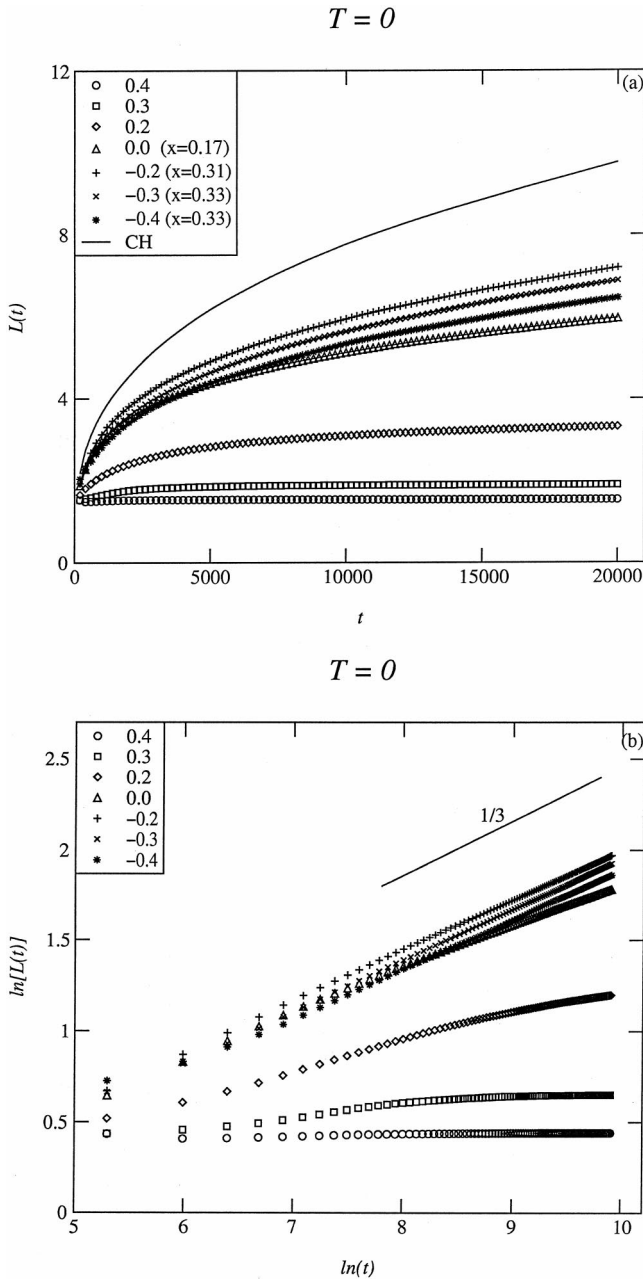


FIG. 4. (a) Time dependence of characteristic length scale  $L(t)$  vs  $t$  for the deterministic ( $T=0$ ) evolution of our model. We present results for  $\psi_0=0.4,0.3,0.2,0.0,-0.2,-0.3,-0.4$ —denoted by the specified symbols. In each case, we attempted to fit the numerical data to the power-law form,  $L(t)=a+bt^x$ , and the best-fit lines (wherever a fit was possible) are superposed on the relevant data sets. The corresponding best-fit exponents are specified in the figure. The error bars on these exponents are  $\pm 0.01$ . For reference, the solid line denotes length-scale data from a simulation of the Cahn-Hilliard (CH) equation, i.e., Eqs. (24)–(25) with  $h(\psi)=1$  and  $\epsilon=0$ . (b) Plot of  $\ln[L(t)]$  vs  $\ln t$  for the data from (a). The solid line has a slope  $1/3$  and refers to the Lifshitz-Slyozov (LS) growth law.

process. Our results in this paper present an alternative explanation, which may be relevant in some experiments. In general, the presence of a low-mobility percolated matrix suppresses diffusion and disables the evaporation-

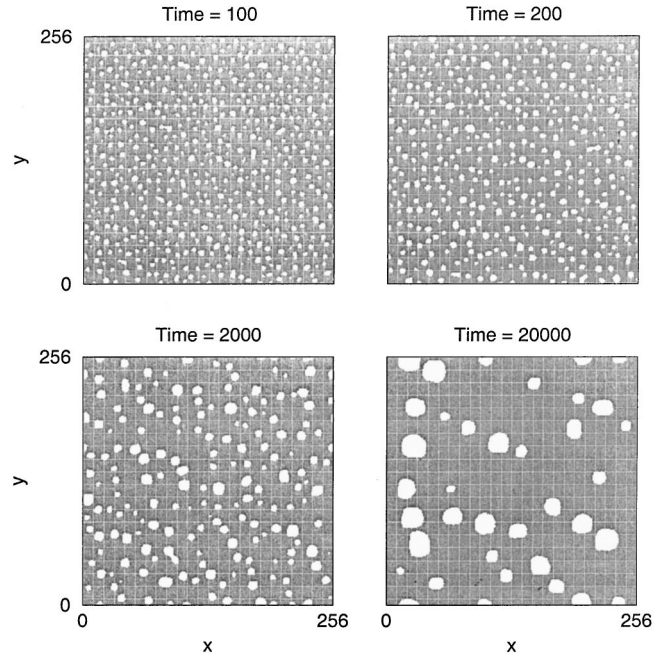


FIG. 5. Analogous to Fig. 1, but with thermal fluctuations included. The amplitude of thermal noise corresponding to this simulation was  $\epsilon=0.1$ .

condensation mechanism for phase separation. However, thermal fluctuations restore a LS-like growth law through the Brownian coalescence mechanism. Clearly, deep quenches suppress thermal fluctuations and also disable the Brownian coalescence mechanism—thereby resulting in microstructure formation in coarsening polymer-solvent mixtures.

### V. SUMMARY AND DISCUSSION

Let us conclude this paper with a brief summary and discussion of the results presented here. We have formulated a

$$\psi_0 = 0.3$$

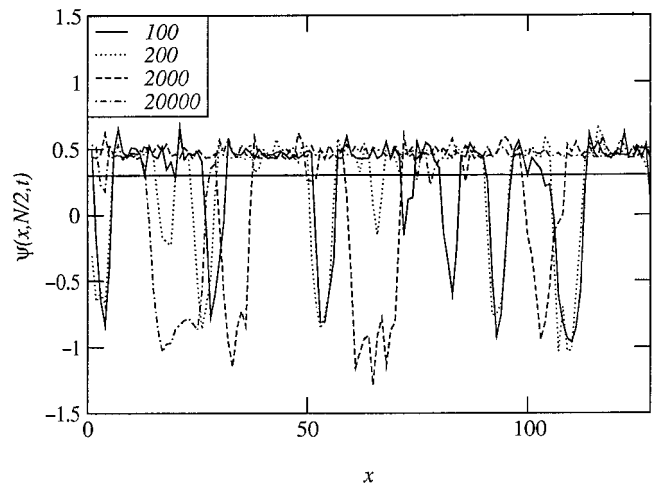


FIG. 6. Analogous to Fig. 2, but for the evolution pictures in Fig. 5.



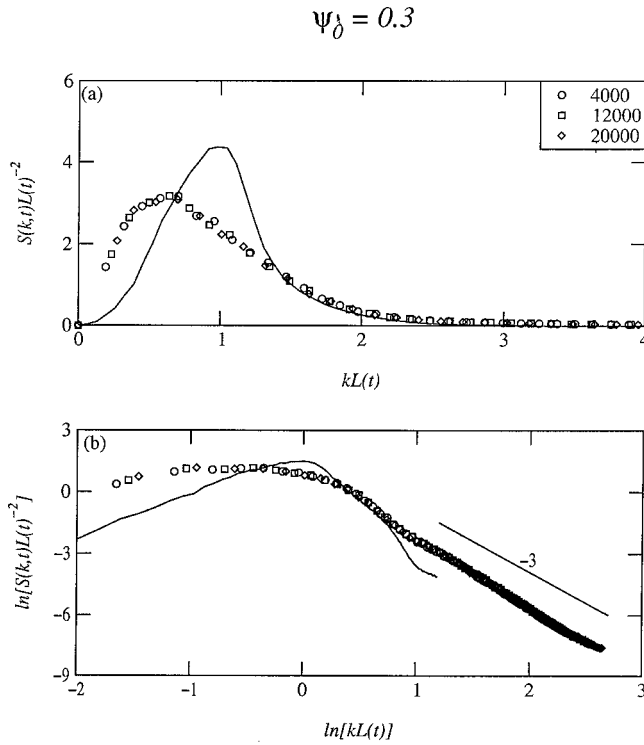


FIG. 7. Analogous to Fig. 3, but for the noisy evolution depicted in Fig. 5. The solid lines in (a) and (b) denote the  $t=20\,000$  data for the  $T=0$  case shown in Fig. 3.

simple dynamical model for phase separating polymer-solvent mixtures, where the polymer-rich region undergoes gelation. This model considers the coupled dynamics of two-order parameters: (a) conserved kinetics for the polymer density field; and (b) nonconserved kinetics for the chemical bond field, which models the possibility of a bond between monomers on neighboring sites. We are interested in the physically relevant limit, where the time scale of gelation is much faster than the time scale of phase separation. In this limit, our dynamical model reduces to the usual CH model for phase separation—generalized to include an order-parameter-dependent mobility, which is set to zero in the gel phase.

Our modeling does not explicitly account for hydrodynamic effects. Nevertheless, we expect our results to apply in that context also, because hydrodynamic modes are not relevant for phase separation in the strongly off-critical quenches considered here. In general, these modes only become relevant when the coarsening system has a bicontinuous domain morphology [1]. Furthermore, even for bicontinuous morphologies, we expect high-viscosity gel-rich regions to strongly dampen fluid velocity fields.

Our primary interest in this paper is the effect of thermal fluctuations on phase separation in these polymer-solvent mixtures. To the best of our knowledge, there is no standard prescription for the incorporation of thermal noise in models with order-parameter-dependent mobility. Therefore, we employ a straightforward generalization of the usual prescription, which is justifiable in special cases [22,23]. As we are interested in the far-from-equilibrium problem of phase separation,

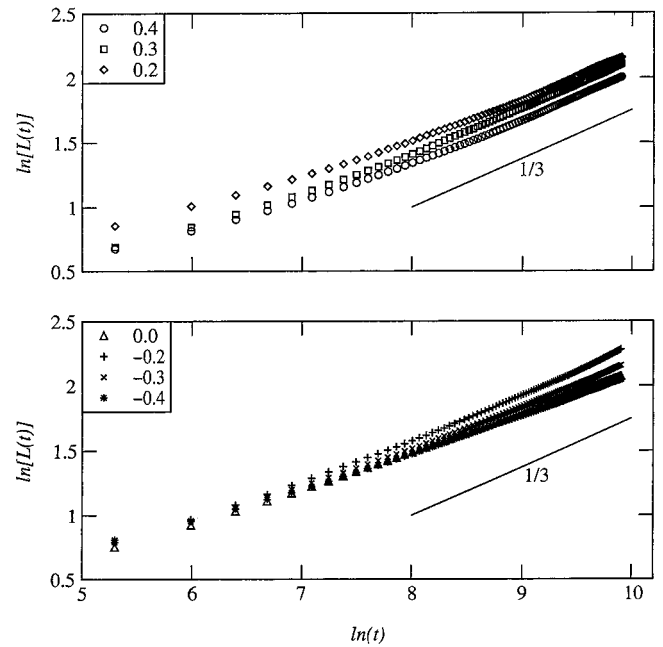


FIG. 8. Analogous to Fig. 4(b), but for evolution with thermal fluctuations. For clarity, the upper frame shows data for  $\psi_0 = 0.4, 0.3, 0.2$ ; and the lower frame shows data for  $\psi_0 = 0.0, -0.2, -0.3, -0.4$ . The solid line in both frames has a slope of  $1/3$ , and refers to the LS growth law.

ration, we believe that this generalization is reasonable in that context.

We have studied the growth of initial fluctuations about a homogeneous high-temperature state, subsequent to a quench. The gelation process amplifies the growth of initial fluctuations because it is energetically and entropically favorable for monomers to aggregate and form chemical bonds. In the context of linearized theory, we have quantified the time scales of growth of fluctuations in terms of experimentally measurable parameters.

Subsequent to the linearized regime, the effects of nonlinearity and the order-parameter-dependent mobility become relevant. In the absence of thermal fluctuations, the phase-separating system “freezes” into a microstructure (or slows down drastically) when the gel phase percolates the system—due to suppression of the evaporation-condensation mechanism for phase separation. However, in the presence of thermal fluctuations, phase separation is enabled by the Brownian motion and coalescence of droplets. The corresponding growth law is similar to the Lifshitz-Slyozov law, i.e.,  $L(t) \sim t^{1/3}$ . We believe that our results provide an alternative explanation for the experimental observation that pinning in phase-separating polymer-solvent mixtures occurs only for low-temperature quenches [6].

We are presently interested in investigating the effects of thermal noise on freezing (or slow growth) in models of polymer-solvent mixtures where the elastic energy has been explicitly accounted for [17]. It seems plausible that Brownian coalescence processes will also play an important role in that context.

## ACKNOWLEDGMENTS

S.P. is grateful to R. Bansil, R. Bausch, H. Bohidar, D.S. Dean, J. Jackle, A. Onuki, S. Ramaswamy, R. Schmitz, K. Sekimoto and H.E. Stanley for useful discussions. In particu-

lar, he would like to acknowledge much useful input from D. S. Dean and S. Ramaswamy regarding the incorporation of noise in systems with order-parameter-dependent mobility. J.S. acknowledges financial support from the University Grants Commission, India.

- 
- [1] For reviews, see K. Binder, in *Materials Science and Technology*, Phase Transformations in Materials Vol. 5, edited by R. W. Cahn, P. Haasen and E. J. Kramer (VCH, Weinheim, 1991), p. 405; A. J. Bray, *Adv. Phys.* **43**, 357 (1994).
- [2] K. Binder and D. Stauffer, *Phys. Rev. Lett.* **33**, 1006 (1974); *Z. Phys. B* **24**, 406 (1976).
- [3] I. M. Lifshitz and V. V. Slyozov, *J. Phys. Chem. Solids* **19**, 35 (1961).
- [4] (a) For studies with quenched disorder, see S. Puri, D. Chowdhury, and N. Parekh, *J. Phys. A* **24**, L1087 (1991); S. Puri and N. Parekh, *ibid.* **25**, 4127 (1992); M. F. Gyure, S. T. Harrington, R. Strilka, and H. E. Stanley, *Phys. Rev. E* **52**, 4632 (1995); (b) for studies with annealed disorder, see S. Puri, *Phys. Rev. E* **55**, 1752 (1997); S. Puri and R. Sharma, *ibid.* **57**, 1873 (1998).
- [5] For reviews, see G. Krausch, *Mater. Sci. Eng., R* **R14**, 1 (1995); S. Puri and H. L. Frisch, *J. Phys.: Condens. Matter* **9**, 2109 (1997).
- [6] R. Bansil, J. Lal, and B. L. Carvalho, *Polymer* **33**, 2961 (1992); J. Lal and R. Bansil, *Physica A* **186**, 88 (1992); R. Bansil, *J. Phys. IV* **3**, 225 (1993).
- [7] T. Hashimoto, M. Takenaka, and H. Jinnai, *Polym. Commun.* **30**, 177 (1989).
- [8] A. Harada and Q. Tran-Cong, *Macromolecules* **30**, 1643 (1997); Q. Tran-Cong, K. Kataoka, and O. Urakawa, *Phys. Rev. E* **57**, R1243 (1998).
- [9] For example, see L. H. Sperling, *Interpenetrating Polymer Networks and Related Materials* (Plenum, New York, 1981); *Interpenetrating Polymer Networks*, edited by D. Klempner, L. H. Sperling, and L. A. Utracki, ACS Series on Advances in Chemistry (ACS, Washington, DC, 1994), Vol. 239.
- [10] P.G. de Gennes, *J. Phys. (France) Lett.* **40**, L69 (1979).
- [11] A. Derouiche, A. Bettachy, M. Benhamou, and M. Daoud, *Macromolecules* **25**, 7188 (1992).
- [12] J. Chikina and M. Daoud, *J. Chem. Phys.* **107**, 5948 (1997).
- [13] A. Brulet, M. Daoud, P. Zhou, and H. L. Frisch, *J. Phys. II* **3**, 1161 (1993).
- [14] F. Sciortino, R. Bansil, H. E. Stanley, and P. Alstrom, *Phys. Rev. E* **47**, 4615 (1993).
- [15] D. Sappelt and J. Jackle, *Europhys. Lett.* **37**, 13 (1997); *Physica A* **240**, 453 (1997); *Polymer* **39**, 5253 (1998).
- [16] K. Sekimoto, N. Suematsu, and K. Kawasaki, *Phys. Rev. A* **39**, 4912 (1989).
- [17] A. Onuki and S. Puri, *Phys. Rev. E* **59**, R1331 (1999).
- [18] A. Onuki, *J. Phys. Soc. Jpn.* **57**, 699 (1988); *Phys. Rev. A* **39**, 5932 (1989).
- [19] S. C. Glotzer, M. F. Gyure, F. Sciortino, A. Coniglio, and H. E. Stanley, *Phys. Rev. Lett.* **70**, 3275 (1993); *Phys. Rev. E* **49**, 247 (1994).
- [20] A. Coniglio, H. E. Stanley, and W. Klein, *Phys. Rev. Lett.* **42**, 518 (1979); *Phys. Rev. B* **25**, 6805 (1982).
- [21] P. C. Hohenberg and B. I. Halperin, *Rev. Mod. Phys.* **49**, 435 (1977).
- [22] S. Ramaswamy (private communication); D. S. Dean (private communication).
- [23] D. S. Dean, *J. Phys. A* **29**, L613 (1997).
- [24] R. Schmitz and S. Puri (unpublished).
- [25] T. Ohta, *Ann. Phys. (N.Y.)* **158**, 31 (1984).
- [26] E. D. Siggia, *Phys. Rev. A* **20**, 595 (1979).